Journal of Testing and Evaluation, Vol. 39, No. 1
Paper ID JTE102940
Available online at: www.astm.org

D. Ferreño,[1] *S. Cicero,*[2] *I. Carrascal,*[2] *and E. Meng*[3]

Validation Through Finite Element Simulation of the Behaviour of a Polyurethane Shock Absorber Under In-Service and Extreme Conditions

ABSTRACT: The safety rules for the construction and installation of lifts, currently in force in Europe, include several requirements concerning the behaviour of the shock absorbers when stopping an elevator. In this paper, a finite element model simulating the behaviour of a cellular polyurethane shock absorber has been developed. The material mechanical behaviour was simulated by means of an elastomeric foam theoretical model, previously calibrated in a former paper. Several in-service and extreme condition scenarios have been analysed with this numerical model, thus verifying the fulfilment of the requirements of the standard.

KEYWORDS: finite elements, cellular polyurethane elastomer, ABAQUS, dynamic simulation, non-linear behaviour

Introduction

In a previous paper [1], the mechanical response of an elastic cellular polyurethane elastomer was studied by means of several tests, including the uniaxial compressive, planar, volumetric, and simple shear tests. The experimental results made it possible to fit the parameters of various models of mechanical behaviour for hyperelastic and elastomeric foam materials and, hence, to select the most adequate for describing the mechanical behaviour of this polyurethane. From this experimental and analytical work, the so-called "elastomeric foam model" was selected, and its material parameters were estimated by means of a least-squares fitting procedure.

The standards UNE-EN 81-1:2001, UNE-EN 81-2:2001/A1, and UNE-EN 81-3:2001 [2–4] (Safety Rules for the Construction and Installation of Lifts), currently in force in Europe, classify the buffers into the category of "energy accumulative shock absorbers." According to Refs 2–4, these elements must fulfill the next set of requirements in the hypothetical situation in which an elevator impacts against the buffer with a velocity 15 % higher than the nominal velocity.

- The average deceleration during the braking must be less than 1*g* (*g* being the acceleration of gravity, i.e., $g = 9.8\ \mathrm{m/s^2}$).
- The acceleration 2.5*g* must be overtaken for a time not longer than 0.04 s.
- The returning velocity of the cabin should not exceed 1 m/s.
- No permanent deformation must remain in the buffer after the impact.

Manuscript received December 28, 2009; accepted for publication June 11, 2010; published online July 2010.

[1]Laboratorio de la División de Ciencia e Ingeniería de los Materiales (LADICIM), E.T.S. de Ingenieros de Caminos, Canales y Puertos, Univ. de Cantabria, Av. Los Castros s/n, 39005 Santander, España (Corresponding author), e-mail: ferrenod@unican.es

[2]Laboratorio de la División de Ciencia e Ingeniería de los Materiales (LADICIM), E.T.S. de Ingenieros de Caminos, Canales y Puertos, Universidad de Cantabria, Av. Los Castros s/n, 39005 Santander, España.

[3]Ascensores Amuesa Polígono Industrial Raos, Parcela 13H, Maliaño, 39600 Santander, España.

Aims of the Present Work

In many cases, it seems inaccessible to empirically verify the requirements mentioned above from both practical and economic points of view. For this reason, in this paper, an alternative methodology is proposed in which the results of the mechanical characterisation collected in Ref 1 were implemented in a finite element (FE) model of the component (see Fig. 1) in order to check the requisites imposed by European standards [2–4]. The relevant geometrical dimensions of the buffer (which are detailed in Ref 1) are a height of 200 mm and an external diameter of 125 mm.

The sequence of actions followed is next summarised:

- The mechanical behaviour of the material was represented, as demonstrated in Ref 1, by means of an elastomeric foam form with the set of material parameters obtained in that previous paper. The strain-energy (per unit of undeformed volume) potential function of elastomeric forms corresponds to expression 1

$$U = \sum_{i=1}^{N} \frac{2\mu_i}{\alpha_i^2}\left[\hat{\lambda}_1^{\alpha_i} + \hat{\lambda}_2^{\alpha_i} + \hat{\lambda}_3^{\alpha_i} - 3 + \frac{1}{\beta_i}\left((J^{\mathrm{el}})^{-\alpha_i\beta_i} - 1\right)\right] \quad (1)$$

  where: N, μ_i, α_i, and β_i=material parameters (the last three, temperature dependant) to be fitted through a least-squares-fit procedure.

N must be chosen a priori by the user. The fitting parameters and the root mean square error obtained in Ref 1 are summarised in Table 1.

- This model with its fitting parameters has been implemented in a FE numerical model developed to reproduce the response of the buffer under different representative conditions.
- The FE model has been validated experimentally by reproducing a dynamic condition on the buffer and comparing the empirical response with the numerical predictions.
- Once the FE model has been validated, additional simulations with the conditions imposed by Ref 2–4, mentioned in the Introduction, have been generated, thus allowing the fulfilment of the standard requirements to be verified.

FIG. 1—*Photograph of the buffer shock absorber.*

- In addition, the behaviour of the buffer under a hypothetical extreme situation has also been studied by means of the numerical model.

General Description of the Finite Element Model

The FE simulations here developed can be considered highly non-linear since the three possible sources of non-linearity [5–9] must be considered for a reliable analysis. In fact, the impact of an elevator on the buffer shock absorber implies the existence of geometrical non-linearity, which is a consequence of the great deformation of the component; therefore, the equilibrium equations must be established on the actual geometry rather than on the original geometry. Material non-linearity is also present due to the intrinsic response of the material when being compressed. Finally, the contact conditions between the elevator and the buffer represent a high loss of linearity.

In addition, as an impact situation will be simulated, the dynamic conditions must be taken into consideration. In general, two different numerical approaches can be used in a FE problem, namely, the implicit and the explicit ones. The former is recommended when performing a quasi-static analysis with not very complex contact conditions. In contrast, for analysis of transient dynamic events, such as impact, or highly non-linear problems involving changing contact conditions, an explicit dynamic FE formulation is recommended [5]. Under these conditions, the implicit method is clearly disadvantageous as, for an accurate simulation, very small increments should be used, thus leading to extremely expensive calculations. The FE software ABAQUS [5] consists of two main different packages, ABAQUS/Standard and ABAQUS/Explicit; the former is based on implicit techniques while the latter uses explicit formulation. For these reasons, in this work, ABAQUS/Explicit has been used.

The buffer absorber includes two different materials, the polyurethane foam (modelled as elastomeric foam, see Ref 1, as mentioned above) and the cast iron of the basis of the component (a 5 mm thick cylindrical steel plate), which is joined to the foam (see Fig. 1). This cast iron was modelled as a linear-elastic material with a Young modulus $E=200$ GPa and a Poisson ratio $v=0.2$.

TABLE 1—*Fitting parameters and RMSE obtained in Ref 1 by modelling the material response as an elastomeric foam form.*

	$i=1$	$i=2$	$i=3$
μ_i	−6.488	7.37	−0.1436
α_i	3.121	3.423	9.816
β_i	0.1874	0.1765	0.5758
RMSE (%)	25.94		

Taking into consideration the symmetry of the problem, an axisymmetric two-dimensional model would be sufficient to perform the analysis; however, for facilitating the circumferential stresses to be obtained, a three-dimensional (3D) FE model was built. Moreover, the original scope of the research included some non-symmetric actions on the buffer that implies the use of a 3D model of the part.

The ABAQUS Explicit solid element library [5] includes first order (linear) as well as second order (quadratic) interpolation elements. In addition, reduced integration, hybrid, and incompatible mode elements are available. Choosing an element for a particular analysis can be simplified by considering specific element characteristics: First or second order; full or reduced integration; hexahedra or tetrahedral; or normal, hybrid, or incompatible mode formulation. For the purposes of this research, the C3D8 element was chosen. It consists of a 3D continuum brick element, with eight nodes (one in each of the vertexes of the brick) and first order interpolation. The hexahedra were chosen because, in general, they have better convergence rate than tetrahedral and, in this case, the simple shape here analysed allows the part to be meshed with no difficulties. Full integration was chosen as it generally yields more accurate results than the reduced integrated elements; moreover, the possibility of hourglassing distortions in the mesh is avoided with full integration techniques.

Experimental Results on the Shock Absorber

To validate the predictions of the FE model developed here (in which the material parameters obtained in Ref 1 have been implemented), two different tests have been performed on the component: First, a quasi-static compressive test and, second, a dynamic test. The second test has been used for the validation, whereas the comparison between the response of the buffer under quasi-static and dynamic conditions should allow the detection of any influence of the loading rate on the mechanical behaviour. The tests have been performed in a universal INSTRON 8501 hydraulic machine (able to work also under static or dynamic regime) with a load capacity of 100 kN. In both cases, to minimise the barrel formation, frictionless test conditions have been provided by means of a thin lubricant layer on the upper surface of the buffer.

Uniaxial Quasi-Static Compression Test on the Buffer

Figure 2 shows the experimental arrangement of the quasi-static test: The buffer, as can be appreciated, is positioned between the supporting and the loading plates. The test is performed under displacement control conditions, with the crosshead velocity set to 0.1 mm/s for an approximate nominal strain rate of 5×10^{-4} s^{-1}. The load versus displacement curve is shown in Fig. 3.

FIG. 2—*Photograph of the experimental arrangement to test the buffer under quasi-static uniaxial regime.*

Uniaxial Dynamic Compression Test on the Buffer

The experimental arrangement shown in Fig. 2 has also been used for the dynamic test. It is worth noting that, in practice, it is difficult to reach fully dynamic conditions since the INSTRON 8501 crosshead velocity is limited in a displacement control ramp. To avoid this inconvenience, a different condition has been imposed for the test by applying a "control displacement square wave" to the buffer, as shown in Fig. 4, where the displacement imposed is represented against time. The "square wave" consists of an initial 90 mm compressive displacement ramp in ~0.63 s, holding up this position for 1.37 s and finishing with an unloading in ~0.58 s.

With these conditions, a crosshead velocity of 143 mm/s is reached (or, equivalently, an approximate nominal strain rate of 0.7 s^{-1}), which means an increase higher than three orders of magnitude with respect to the quasi-static conditions (see the Uniaxial Quasi-Static Compression Test on the Buffer section). On the other hand, it must be remembered that the nominal speed in an elevator is about 1 m/s; therefore, the gap between the maximum experimental rate (143 mm/s) and the nominal operative rate in an elevator (≈1 m/s) is less than one order of magnitude. Therefore, it will

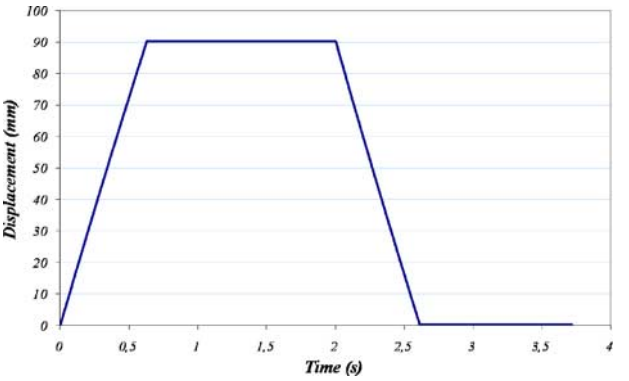

FIG. 4—*Control displacement square wave imposed on the buffer.*

be assumed that this gap is narrow enough to neglect any loss in reliability once the FE model has been validated for the experimental conditions.

The experimental results of this dynamic test, load versus displacement curve, can be appreciated in Fig. 5, where an evident oscillating noise is superimposed on the main curve due to the dynamic regime. On the other hand, the complete displacement recovery after unload is clear, which confirms the fulfilment of one of the requirements in Refs 2–4, as stated in the Introduction.

A comparison between the quasi-static and dynamic behaviour is also present in the figure. In principle, two sources for dynamic effects could be distinguished: First, the inertial effects, not foreseeable in this context, for the reduced values of the density of the polyurethane (400 kg/m^3) and size of the buffer; second, the possible intrinsic dependence of material properties on loading rate. The comparison in Fig. 5 allows establishing that since the curves almost superimpose each other, no dynamic effect on the material is expected, at least for the rates here considered.

Validation of the Finite Element Model

The goal of this section is to validate the numerical model developed in order to, in the next stage (the Numerical Evaluation of Operation Conditions section), simulate the real behaviour of an in-service elevator, verifying the fulfilment of the conditions imposed in the standards [2–4] stated in the Introduction. For this purpose, the experimental dynamic scenario described in the Experi-

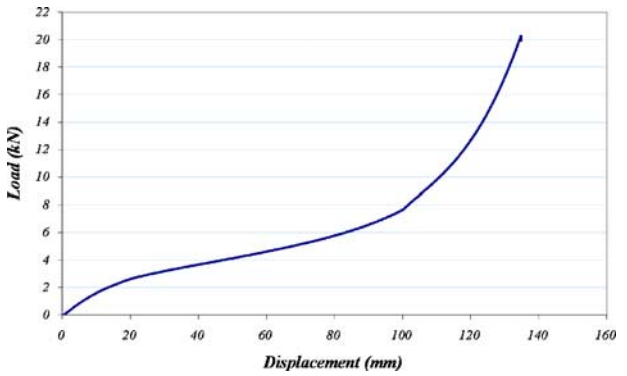

FIG. 3—*Load versus displacement curve obtained from the uniaxial quasi-static compression test on the buffer.*

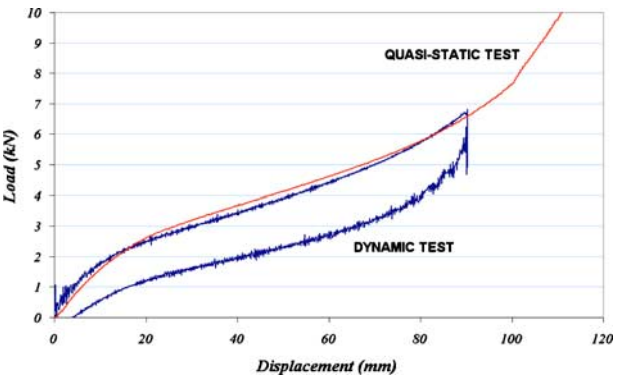

FIG. 5—*Comparison between the quasi-static (Fig. 3) and dynamic uniaxial compression tests.*

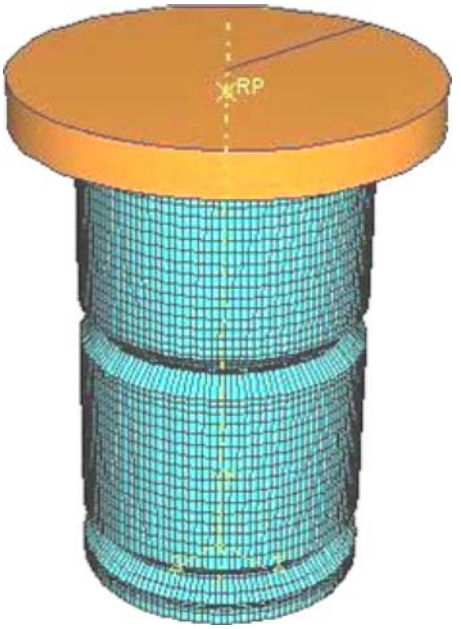

FIG. 6—*Geometry of the FE model of the buffer.*

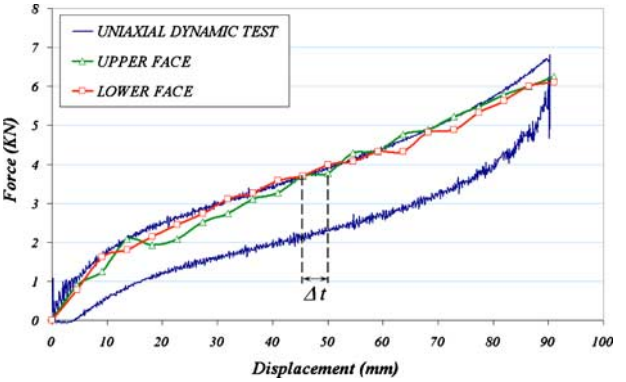

FIG. 7—*Comparison between experimental and numerical curves under dynamic conditions.*

mental Results on the Shock Absorber section has been reproduced by means of FE.

In Fig. 6, a perspective of the numerical model of the buffer can be appreciated. The boundary conditions consist of a displacement imposed on the (rigid solid) upper plate (which plays the role of the elevator) according to the initial ramp in Fig. 4 (90 mm in ~0.63 s at constant rate), whereas the lower surface of the component (the steel plate of the buffer) was vertically fixed. Taking into consideration the experimental conditions stated above, a frictionless contact was imposed between the upper plate and the buffer.

The contact force in the upper surface of the buffer and the reaction force in its base have been obtained and are represented in Fig. 7, where the experimental curve of Fig. 5 (dynamic test) has also been included. In general, there is good agreement between the numerical and experimental results (mainly taking into consideration the intrinsic difficulties of a dynamic problem where the three sources on non-linearity, described above, take place).

Several interesting features should be pointed out. It is evident in Fig. 7 how the upper surface receives the impact and, almost instantly, the contact force increases, whereas the reaction force in the lower face shows some delay. The oscillating appearance of both numerical curves is also evident, one being in opposition with the other; Δt represents the period of the oscillation, as seen in the figure, $\Delta t \sim 5$ s. This fact can be interpreted as a consequence of the shock wave propagating in the material after the impact: This is represented in Fig. 8, which shows the stress mapping in different instants of the simulation, during the compression of the buffer. This figure also allows at appreciating the great deformation of the component during the simulation. In order to ensure the correct interpretation of the oscillatory pattern in the FE curves, some further research was developed, as briefly explained hereafter.

The speed of propagation of a wave in a continuum medium is proportional to $(E/\rho)^{1/2}$ [6–9], E being the elastic modulus and ρ being the density of the material. Therefore, the time required by the wave to travel across the buffer from the upper to the lower surface, which is directly related to the delay between signals in Fig. 7, will be inversely proportional to the rate of propagation; therefore, $\Delta t \sim (\rho/E)^{1/2}$. According to this expression, an increase in the density of the material must generate a new response with a higher period in the oscillating signals.

For this reason, in order to justify this oscillating feature, an additional simulation was performed artificially increasing the density of the material one order of magnitude (therefore, ρ

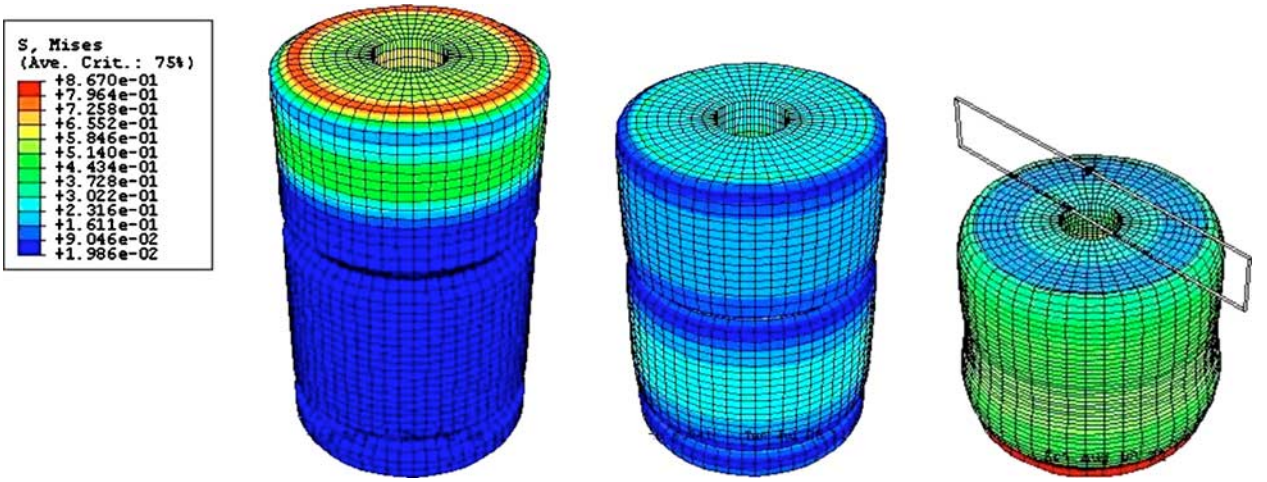

FIG. 8—*Stress mapping in the buffer in different instants of the simulation. A shock wave propagating in the material can be appreciated.*

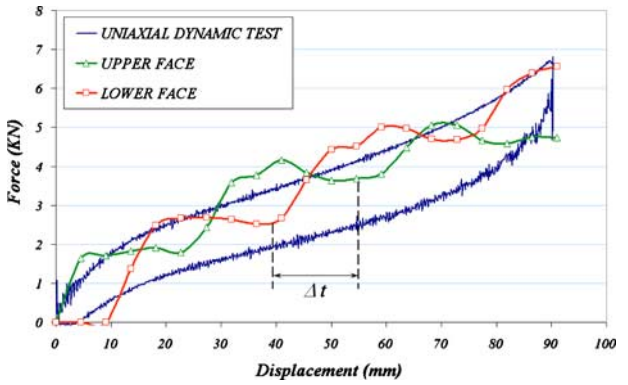

FIG. 9—*Comparison between experimental and numerical curves under dynamic conditions with density increase in the material.*

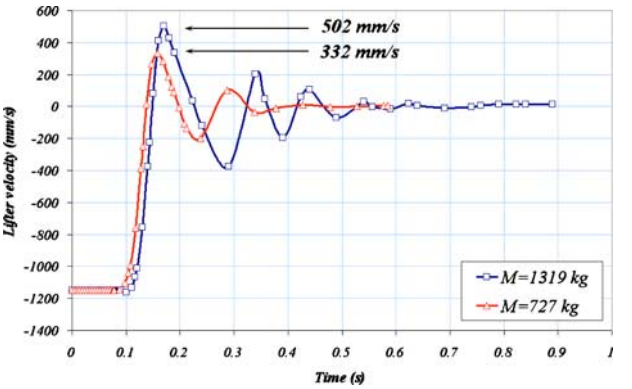

FIG. 10—*Velocity as a function of time (in-service conditions) for M = 1319 kg and M = 727 kg.*

~ 4000 kg/m^3). Figure 9 shows the numerical curves thus obtained, where the predicted increase in Δt is evident. In this case, $\Delta t \sim 15$ s, which is in very good agreement with what could be expected. Of course, the last argument must be taken with care and considered as semiquantitative since the elastomeric foam is not a continuum media but a porous one.

Numerical Evaluation of Operation Conditions

As mentioned above (Introduction), different FE calculations have been performed in order to evaluate the in-service behaviour of the buffer absorber. Two different scenarios have been analysed: On the one hand, the conditions stated in the European standards [2–4] (in-service conditions) and, on the other hand, a free fall of the elevator (here denominated as extreme condition).

Numerical Simulation of In-Service Conditions

According to the standards UNE-EN 81-01:2001, UNE-EN 81-2:2001/A1, and UNE-EN 81-3:2001 [2–4], a nominal velocity $v_n = 1$ m/s must be considered in the elevator and, for calculations, an impact velocity 15 % higher, which yields $v_i = 1.15$ m/s. Moreover, the mass of the elevator must be included in the range of 727–1319 kg; in this work, both extreme cases have been simulated in spite of the evident fact that the worst condition must correspond to the mass $M = 1319$ kg.

From the numerical calculations under these conditions, the velocity and acceleration curves of the elevator (which in the FE model is represented by the mass impacting the buffer; see Fig. 6) as a function of time have been obtained and are represented in Figs. 10 and 11. In both cases ($M = 727$ and 1319 kg), the oscillating pattern of the braking process in the elevator is evident. Figure 10 allows the maximum returning velocity of the elevator to be obtained, yielding 332 mm/s for $M = 727$ kg and 502 mm/s for $M = 1319$ kg. Therefore, the condition stated in the Introduction [2–4] that establishes a limit in the returning velocity of 1 m/s is fulfilled.

In Fig. 11, the acceleration curves are represented. It should be pointed out that since the initial conditions consist of a constant velocity of the elevator, the acceleration before the impact takes place must be zero, as can be appreciated in Fig. 11. It can also be observed that the deceleration $2.5g$ is only exceeded during 0.029 s for a mass $M = 727$ kg and 0.033 s for a mass $M = 1319$ kg. Again, the standard [2–4] condition that establishes a limit time of 0.04 s is satisfied.

Finally, the average deceleration, $\langle a \rangle$, can be obtained in each case through numerical integration of the curves (between two consecutive minima) in Fig. 11. By doing so, the next results are obtained

$$\langle a_{727\ \mathrm{kg}} \rangle = 12.0\ \mathrm{m/s^2} = 1.23g \tag{2}$$

$$\langle a_{1319\ \mathrm{kg}} \rangle = 19.9\ \mathrm{m/s^2} = 2.02g \tag{3}$$

Therefore, the limit $\langle a \rangle = 1g$ is exceeded in both cases. In order to satisfy this requirement, two improvements are here proposed. First is to increase the length of the buffer in order to achieve a softer arresting of the elevator; this solution has the evident inconvenience of needing the fabrication of a completely new component, which could result extremely expensive. Therefore, a second solution is proposed, to reduce the weight of the elevator supported by each of the buffer absorbers or, equivalently, to increase the number of buffer absorbers for a lifter. This second option can easily be applied in practice, with no relevant cost increase, as this kind of buffers represents an economical solution (see Ref 1).

Numerical Simulation of Extreme (Free Fall) Conditions

A second structural application for the FE model here developed has been studied. It consists of a hypothetical situation in which the elevator with $M = 1319$ kg falls freely from the (small) height, h, that corresponds with an impact velocity $v_i = 1.15$ m/s, equal to

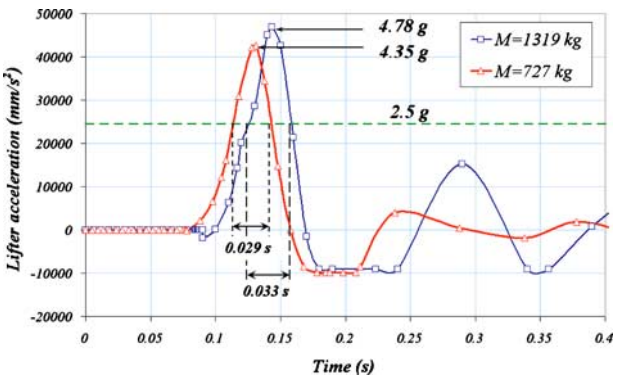

FIG. 11—*Acceleration of the elevator as a function of time (in-service conditions) for M = 1319 kg and M = 727 kg.*

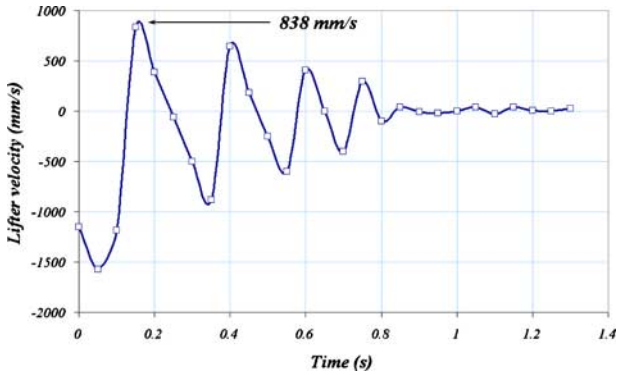

FIG. 12—*Graph of velocity as a function of time (M = 1319 kg) under free fall conditions.*

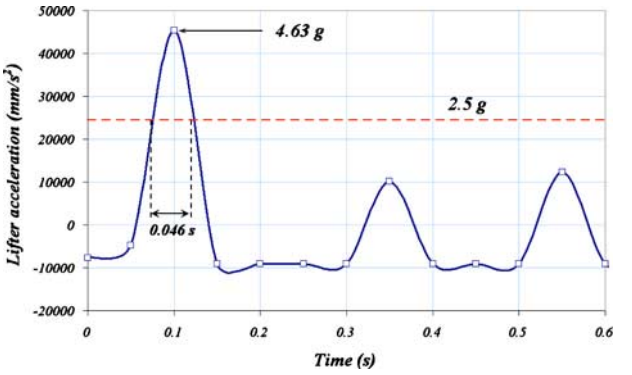

FIG. 13—*Graph of acceleration as a function of time (M = 1319 kg) under free fall conditions.*

that used in the Numerical Simulation OF In-Service Conditions section. This height can be easily calculated by equating the potential energy (mgh) with the kinetic energy ($mv^2/2$); this yields the result $h = 6.7$ cm.

With these conditions, the influence of gravity can be evaluated. As before, the velocity and acceleration curves have been obtained and are represented in Figs. 12 and 13. The velocity curve clearly reveals that the impact in this case is much more violent, the maximum returning velocity being 838 mm/s. The maximum acceleration is (see Fig. 13) 4.63g, similar to those shown in Fig. 11; nevertheless, in this case the initial acceleration ($-g$) must be considered, the total change in acceleration being 5.63g.

Finally, as shown in Fig. 13, the limit 2.5g is exceeded during 0.046 s, clearly out of the limit established in Refs 2–4. These results reveal the great importance of security systems in elevators (such as emergency brakes or governors) that avoid free fall impacts, ensuring constant velocity conditions during accidents. Without these complementary elements, the use of buffers or other kind of shock absorbers would be presumably useless, even with small falling heights, as demonstrated above.

Conclusions

In this paper, a detailed numerical study of the behaviour of a shock absorber under in-service and extreme conditions has been performed. For this purpose, the results regarding the mechanical behaviour of the material (a cellular polyurethane elastomer, characterised in Ref 1) have been taken into account. Several conclusions can be drawn.

- The experimental validation of the FE model by reproducing an impact condition has demonstrated that no intrinsic dynamic effect must be considered in the material.
- The dynamic test has made it possible to verify that no permanent deformation remains in the buffer after an impact, as required by European standards [2–4].
- The comparison between the experimental results and the numerical predictions allows the representativeness of the technique here developed to be established.
- The simulation of in-service conditions allowed the rest of requirements of the standard to be verified: In this case, only the requisite concerning the average acceleration during the braking has not been fulfilled. Increasing the number of buffer absorbers is proposed as an inexpensive solution to satisfy this requirement.
- Finally, the numerical simulation of the buffer behaviour under a hypothetical extreme situation has shown the importance of the complementary security systems in order to guarantee the safety and comfort of the passengers.

References

[1] Ferreño, D., Carrascal, I., Cicero, S., and Meng, E., "Characterization of Mechanical Properties of a Shock Absorber Polyurethane Foam for Elevators. Numerical Fitting of Mechanical Behavior Models for Hyperelastic and Elastomeric Foam Materials," *J. Test. Eval.*, Vol. 38, No. 2, pp. 211–221.

[2] UNE-EN 81-1:2001, 2006, "Safety Rules for the Construction and Installation of Lifts; Part 1: Electric Lifts; A2: Machinery and Pulley Spaces," AENOR, Madrid.

[3] UNE-EN 81-2:2001/A1, 2006, "Safety Rules for the Construction and Installation of Lifts-Part 2: Hydraulic Lifts," AENOR, Madrid.

[4] UNE-EN 81-3:2001, 2001, "Safety Rules for the Construction and Installation of Lifts. Part 3: Electric and Hydraulic Service Lifts," AENOR, Madrid.

[5] Hibbit, D., Karlsson, B., and Sorensen, P., *ABAQUS Analysis User's Manual; Version 6.5.* (2004). HKS Inc., Pawtucket, RI, Vol. 3.

[6] Malvern, L. E., *Introduction to the Mechanics of a Continuous Medium*, Prentice-Hall, Inc., Englewood Cliffs, NJ, 1969.

[7] Barbat, A. H. and Canet, J. M., *Estructuras Sometidas a Acciones Sísmicas. Cálculo por Ordenador [Seismic Actions on Structures. Computer Calculations]*, 2nd ed., Centro Internacional de Métodos Numéricos en Ingeniería, Barcelona, 1994, ISBN: 84-87867-10-3.

[8] Zienkiewicz, O. C. and Taylor, R. L., *The Finite Element Method Set*, 6th ed., Butterworth-Heinemann, Burlington, MA, 2005, ISBN-13: 978-0750664318.

[9] Avilés, R. and Goizalde, M. B., *Análisis Dinámico Mediante Elementos Finitos*, ETS de Ingenieros, Bilbao, 1995, ISBN 84-600-9213-5.